



Vertical cell movement is a primary response of intertidal benthic biofilms to increasing light dose

Rupert G. Perkins, Johann Lavaud, Joao Serôdio, Jean-Luc Mouget, Paolo Cartaxana, Philippe Rosa, Laurent Barillé, Vanda Brotas, Bruno Jesus

► To cite this version:

Rupert G. Perkins, Johann Lavaud, Joao Serôdio, Jean-Luc Mouget, Paolo Cartaxana, et al.. Vertical cell movement is a primary response of intertidal benthic biofilms to increasing light dose. *Marine Ecology Progress Series*, 2010, 416, pp.93-103. 10.3354/meps08787 . hal-01095756

HAL Id: hal-01095756

<https://hal.science/hal-01095756>

Submitted on 16 Dec 2014

HAL is a multi-disciplinary open access archive for the deposit and dissemination of scientific research documents, whether they are published or not. The documents may come from teaching and research institutions in France or abroad, or from public or private research centers.

L'archive ouverte pluridisciplinaire **HAL**, est destinée au dépôt et à la diffusion de documents scientifiques de niveau recherche, publiés ou non, émanant des établissements d'enseignement et de recherche français ou étrangers, des laboratoires publics ou privés.

**Vertical cell movement is a primary response of intertidal benthic biofilms to
increasing light dose**

Perkins, R.G.^{*1}, Lavaud, J.², Serôdio, J.³, Mouget, J-L.⁴; Cartaxana, P.⁵, Rosa, P.⁶, Barille,
L.⁶, Brotas, V.⁵, Jesus, B.M.^{5,7}

* corresponding author

*1. School of Earth, Ocean and Planetary Sciences, Cardiff University, Main Building,
Park Place, CF10 3YE Cardiff, UK E-mail: PerkinsR@cf.ac.uk, Tel.: +44-29-20874943,
Fax: +44-29-20874326

2. UMR CNRS 6250 'LIENSs', Institute for Coastal and Environmental Research (ILE),
University of La Rochelle, 2 rue Olympe de Gouges, 17042 La Rochelle Cedex, France.

3. Departamento de Biologia, Universidade de Aveiro, Aveiro, 3810-193, Portugal

4. Laboratoire de Physiologie et Biochimie Végétales, Faculté des Sciences et
Techniques, Université du Maine, EA2663, Av. O. Messiaen, 72085 Le Mans Cedex 9,
France

5. Centro de Oceanografia, Faculdade de Ciências da Universidade de Lisboa, 1749-016
Lisboa, Portugal.

6. Université de Nantes, EA 21 60 "Mer Molécules Santé", Faculté des Sciences et
Techniques, 2, rue de la Houssinière, BP 92 208, 44322 Nantes cedex 3, France

7. Centro de Biodiversidade, Genómica Integrativa e Funcional (BioFIG), Faculdade de
Ciências, Universidade de Lisboa, Lisboa, Portugal

Abstract

Intertidal soft sediment microphytobenthic biofilms are often dominated by diatoms which are able to regulate their photosynthesis by physiological processes (e.g. down regulation through the xanthophyll cycle, referred to as non-photochemical quenching, NPQ) and behavioural processes (e.g. vertical cell movement in the sediment – biofilm matrix). This study investigated these two processes over a 6 h emersion period using chemical inhibitors under two light treatments (ambient light and constant light at $300 \mu\text{mol m}^{-2} \text{ s}^{-1}$). Latrunculin A (Lat A) was used to inhibit cell movement and dithiothreitol (DTT) to inhibit NPQ. HPLC analysis for chlorophyll *a* and spectral analysis (Normalised Difference Vegetation Index, NDVI) indicated that Lat A significantly inhibited cell movement. Photosynthetic activity was measured using variable chlorophyll fluorescence and radiolabelled carbon uptake and showed that the non-migratory Lat A treated biofilms were severely inhibited as a result of the high accumulated light dose (significantly reduced maximum relative electron transport rate, $r\text{ETR}_{\text{max}}$, and light utilization coefficient, α) compared to the migratory DTT and control treated biofilms. No significant patterns were observed for ^{14}C data, although a decrease in uptake rate was observed over the measurement period. NPQ was investigated using HPLC analysis of xanthophyll pigments (Diatoxanthin, DT and the percentage de-epoxidation of Diadinoxanthin, DD), chlorophyll fluorescence (change in maximum fluorescence yield) and the second order spectral derivative index (Diatoxanthin Index, DTI). Patterns between methods varied, but overall data indicated greater NPQ induction in the non-migratory Lat A treatment and little or no NPQ induction in the DTT and control treatments. Overall the data resulted in two main conclusions: firstly the primary

response to accumulated light dose was vertical movement, which when inhibited resulted in severe down regulation / photoinhibition; secondly diatoms down regulated their photosynthetic activity in response to accumulated light dose (e.g. over an emersion period) using a combination of vertical migration and physiological mechanisms, which may contribute to diel and/or tidal patterns in productivity.

Keywords: benthic, diatom, down regulation, migration, photophysiology, productivity

Introduction

Microphytobenthic biofilms at the surface of intertidal estuarine sediments are highly productive (Brotas and Catarino, 1995; MacIntyre et al., 1996; Underwood and Kromkamp, 1999). The regulatory mechanisms controlling the magnitude and periodicity of this productivity are partly understood as involving sun angle and tidal patterns (Pinckney and Zingmark, 1991) as well as changes in light dose exposure (Kromkamp et al., 1998; Serôdio and Catarino, 1999; Perkins et al. 2002, Jesus et al. 2005). For the latter it has been hypothesised (Kromkamp et al., 1998; Serôdio and Catarino, 1999; Perkins et al. 2002; Jesus et al., 2006a) that cells optimise their position within the surface layers of a sediment biofilm, utilising sediment light attenuation to provide an optimal light environment; this is the concept of microcycling. The importance of vertical movement to regulate light exposure has recently been demonstrated thoroughly using chemical inhibition of movement (Cartaxana and Serôdio, 2008; Cartaxana et al. 2008). However, this is the first study to directly compare the roles of vertical movement, a behavioural form of photosynthetic down regulation (e.g. Perkins et al. 2002), with physiological down regulation in the form of non-photochemical quenching (NPQ; e.g. Lavaud, 2007). Effectively diatom cells move vertically through the sediment matrix utilising extracellular polymers in response to changes in light environment: too much light, cells move downwards, not enough light, cells move upwards. This is a simplification however as the cumulative effect of light exposure over time modifies this response (Perkins et al. 2002, 2006; Jesus et al., 2006b). It should be emphasised as well, that this microcycling movement over short time scales is distinct from the bulk movements of cells as vertical migration (Underwood and Kromkamp, 1999; and see the review by Consalvey et al.,

2004) driven by tidal and sun angle driving forces as originally outlined by Pinkney and Zingmark (1991).

Why do diatom cells require an optimum light environment to maximise their photosynthetic potential? It is well known that excess light can lead to photodamage by production of free radicals and superoxides which may lead to protein breakdown in photosystem II reaction centres, e.g. the D1 dimer (Olaizola et al., 1994; Materna et al., 2009). Cells can hence prevent such damage through two processes, both of which effectively down regulate photosynthetic activity. Firstly, cells can migrate downwards away from high light that could result in a photodamaging light dose. This is effectively a behavioural form of down regulation (Kromkamp et al., 1998; Serôdio and Catarino, 1999; Perkins et al. 2001; Mouget et al., 2008). Secondly cells can down regulate by diverting excess light energy away from PSII reaction centres via alternative energy pathways (Ting and Owens, 1993; Lavaud et al., 2002a; Goss et al., 2006; Lavaud, 2007; Serodio et al., 2008). This physiological process of down regulation is often referred to as non-photochemical quenching (NPQ) as it quenches the energy using energy conversions with no photochemical output. The process utilises energisation of the thylakoid membrane by generation of a proton gradient, which induces de-epoxidation of diadinoxanthin to diatoxanthin (DT) known as the xanthophylls cycle (Lavaud et al., 2002a, 2004, 2007; Goss et al., 2006). DT competes for light energy with chlorophyll pigments in the light harvesting complexes, hence diverting the energy away from the pathway that would lead to generation of harmful reducing agents created by over excitation of PSII reaction centres (Lavaud, 2007; Ruban et al., 2004). Diatoms are known to have highly effective xanthophyll cycle and are able to rapidly induce NPQ in

response to increasing light levels (Goss et al., 2006; Lavaud, 2004, 2007; Ruban et al., 2004; Serodio et al., 2005, 2008) even so far as to induce short term photoacclimation through NPQ induction in the time required for 30 second rapid light curves, e.g. over a 4 minute period (Perkins et al., 2002; Perkins et al., 2006; Cruz and Serodio, 2008).

Diatom cells in surface biofilms can therefore respond to changing light environments, and hence accumulated historical light doses, through two mechanisms, vertical cell movement within the sediment matrix, or NPQ induction. These processes are now well understood, e.g. Consalvey et al. (2004), Kromkamp et al. (1998), Perkins et al. (2002), Spilmont et al. (2007) and Mouget et al. (2008) regarding light induced cell movement and Lavaud (2007) and Perkins et al. 2006 regarding NPQ. Also how does the down regulation effect net productivity and how does this vary in response to the light dose over a low tide emersion period? This study aimed to address these questions through manipulative experiments using engineered biofilms treated with chemical inhibitors, under two different light dose regimes. Chemical treatments comprised inhibition of cell motility using Latrunculin A which inhibits actin filaments involved in diatom movement without affecting photosynthetic activity (Cartaxana et al. 2008) and also the use of DL-dithiothreitol which inhibits the de-epoxidation of DD to DT, and hence inhibits NPQ induction (Lavaud et al., 2002b). These treatments were compared to controls over a 6 hour emersion period under two light treatments, ambient light and a constant low light environment. Thus the roles of cell movement and NPQ induction were compared as functions of the increasing photodose accumulated over the emersion period.

Methods

Experimental design and sampling

Surface mud to a depth of approximately 1 cm was collected on the 1st July 2008 from Alcochete mudflat, located on the eastern shore of the Tagus Estuary (38 44' N, 9 08' W), composed of slightly gravelly mud (Jesus et al 2006c). All experimental measurements were carried out on the following day, 2nd July 2008. The mud and surface biofilm was returned to the laboratory where a sub-sample was examined by light microscopy to determine the dominance of epipellic diatoms in the biofilm. The remainder of the surface mud was thoroughly mixed by hand and then evenly spread in trays to a depth of 5 cm. A shallow depth of site water (< 2 cm) was carefully added so as not to re-suspend the mud and the trays were left overnight in the laboratory. The following morning, at the start of the low tide emersion predicted for the original sample site, the shallow depth of site water was removed and a spectroradiometer (see below) was used to monitor the establishment of surface biomass in one of the sample trays. Plastic cores (2 cm × 2.5 cm diameter) were then carefully inserted into the mud to isolate minicore sediment samples in each sediment tray for the following chemical treatments: controls (addition of filtered site water only), Latrunculin A (Lat A, dissolved in site water) to inhibit cell motility and DL-dithiothreitol (DTT, in site water) to inhibit conversion of DD to DT and hence inhibit non-photochemical quenching (NPQ). Full details of these treatments are given below. Three replicates for each chemical treatment were used to provide independent samples for the following measurement: rapid light response curves using PAM-fluorescence, spectroradiometry, sampling for pigment analysis using HPLC (minicore set 1) and ¹⁴C radiolabelled measurement of primary productivity (minicore set 2). Hence

6 minicores were needed for each treatment for each time sampling point ($n = 3$, T1, 2 and 3 equally spaced 2 h apart). Finally the number of minicores was duplicated in a second sample tray to enable two light treatments to be investigated, ambient light and constant light ($300 \mu\text{mol m}^{-2} \text{s}^{-1}$). Note that all light levels referred to were measured with a Licor cosine corrected light meter and refer to photosynthetically active radiation, 400 – 700 nm. The constant light was provided by a quartz white light source (400W HPI-T Pro Philips). The experimental set up is summarized in Table 1. Ambient light treatment (Amb) and constant low light treatment (Con) were identical other than their respective light dose exposures calculated by integration over time of light measurements taken using a Licor cosine corrected light meter every 30 minutes during the experimental period. Finally, all treatments were applied once the biofilm had established at the sediment surface as assessed by the stabilization of the NDVI reflectance readings; hence chemical and light treatments were applied to established surface biofilms rather than prior to upward cell migration. Measurements using the following methodologies were taken at equal time intervals of 2 h at T1, T2 and T3, hence covering a 6 h exposure period typical for the original sample site. Experiments were carried out under ambient light on the roof of the Instituto de Oceanografia de Lisboa, Lisbon, Portugal. Engineered biofilm trays were incubated in temperature controlled water tanks to minimise potential over-heating (maximum temperatures measured at the sediment surface during the experimental period were 35°C , comparable to those measured in situ). Light dose was calculated for each sampling point T1, T2, T3 by integrating the light measurements (using a Licor cosine corrected light meter) over the preceeding time period.

190 *Chemical preparation and application*

191 Controls – 400 μL of filtered site water was added to all cores to mimic chemical
192 treatments but without addition of DTT or Lat A (see below).

193 DTT - DL-dithiothreitol (Sigma) was prepared as a fresh stock on the morning of the
194 experimental period. A stock solution of 20 mM (in ethanol) was diluted 100 times in
195 freshly filtered site water to reach a final concentration of 200 μM . 400 μL of this
196 solution were added to each core in order to cover the whole surface of the sediment.
197 Given the dimensions of the cores, the amount of DTT added in each core was 0.17
198 μmoles . This amount of DTT was previously determined to be sufficient to virtually fully
199 inhibit the conversion of DD in DT in a 10 $\mu\text{g Chl } a \text{ mL}^{-1}$ suspension *Phaeodactylum*
200 *tricornutum* (100% inhibition with 0.2 $\mu\text{mol DTT}$) (Lavaud et al., 2002b).

201 Latrunculin A - A concentrated Latrunculin A solution (1 mM) was prepared as a fresh
202 stock on the morning of the experimental period by dissolving purified Lat A (Sigma-
203 Aldrich) in dimethylsulfoxide. A solution of 12.5 μM Lat A was prepared by dissolving
204 the appropriate amount of the concentrated stock solution in filtered water collected at the
205 sampling site. Small volumes of this solution (total of 300 μL) were applied to
206 undisturbed sediment samples by carefully pipetting directly onto the sediment surface,
207 until forming a continuous thin layer that completely covered the sample. The amount of
208 Lat A used was previously determined to be sufficient to virtually inhibit diatom
209 migration in benthic biofilms (Cartaxana and Serôdio, 2008). The inhibitor was applied
210 after the formation of the biofilm at the sediment surface during the period coinciding
211 with the beginning of low tide at the sampling site.

212 *Spectral reflectance*

213 Spectral reflectance was measured with a USB2000 (Ocean Optics, Dunedin,
214 USA) with a VIS-NIR optical configuration controlled by a laptop using OOIBase32™
215 software. The spectroradiometer sensor was positioned at a 45° angle pointing at the
216 center of the minicore and measuring an approximate area of 1 cm². Reflectance spectra
217 of the target surface were calculated by dividing the upwelling spectral radiance from the
218 sediment surface (L_u) with the reflectance of a clean white polystyrene plate (L_d) both
219 spectra were corrected for dark noise (D_n) (electronic signal measured at total darkness):

220 (Equation 1)

$$221 \text{ Reflectance} = (L_u - D_n) / (L_d - D_n) \quad (1)$$

222 The polystyrene plates differed less than 3% from a calibrated 99% reflectance
223 standard plate (Spectralon) (Forster and Jesus, 2006). The normalized vegetation index
224 (NDVI) was calculated as follows:

225 (Equation 2)

$$226 \text{ NDVI} = (\text{InfraRed} - \text{Red}) / (\text{InfraRed} + \text{Red}) \quad (3)$$

227 where *InfraRed* is the average reflectance of the range 748-752 nm and *Red* the
228 average reflectance of the range 673-677 nm.

229 Reflectance derived indices are susceptible to background noise and are not
230 sensitive enough to detect the didinoxanthin (DD) to diatoxanthin (DT) pigment
231 conversion that occur during the xanthophyll cycle. Using diatom cultures Jesus et al.
232 (2008) showed that the conversion of DD to DT causes a reflectance decrease at 508 nm
233 is proportional to DT content. However, this decrease was so small that only an index
234 based on the second derivative spectrum was appropriate to detect it. Their DT index
235 (DTI) used the second derivative peak at 508 nm normalized by the second derivative
236 peak at 630 nm and showed very promising results in the determination of diatom DT

content. Thus, DTI was used in the current study as a proxy for the DT present at the sediment surface.

The derivative spectra (δ) were calculated using a finite approximation method (Louchard et al. 2002), after smoothing the reflectance spectra with a natural cubic spline function (60 nodes). The second derivative ($\delta\delta$) was chosen because in theory it eliminates the background effects and strongly enhances minute changes in the reflectance spectra. This would be ideal in intertidal estuarine sediments where the background signal can be strongly influenced by organic matter, sediment type and moisture. The second derivative spectra were only calculated for the ambient light treatment due to the high noise spectra generated by the lamps used in the constant light treatment.

Rapid light response curves

Rapid light response curves were obtained using a Walz Water-PAM fluorimeter and following the methodology of Perkins et al. (2006) except that 20 second light step increments were used rather than 30 seconds due to time constraints. Settings on the Water-PAM were as follows: saturating pulse at setting 10 (approximately $8,600 \mu\text{mol m}^{-2} \text{s}^{-1}$ PAR) for 600 ms duration; light curve settings of 20 second light step duration covering $0 - 1035 \mu\text{mol m}^{-2} \text{s}^{-1}$ PAR (previously determined as adequate to produce fully saturated light curves for biofilms from this site); due to time restrictions during the experimental period, increasing light level steps using the Water-PAM programming were used rather than preferred decreasing light steps using Win Control (Perkins et al., 2006). Light curve measurements were taken in a random order between chemical treatments, however at each time point, ambient light measurements were made prior to

constant light measurements. Once spectral reflectance and fluorescence measurements had been made, the same minicores were destructively sampled for pigment analysis (see below) with care to ensure that the area sampled was not that exposed to the light dose applied by the rapid light curve.

Analysis of rapid light curves also followed that described by Perkins et al. (2006) with curve fitting following the iterative solution of Eilers and Peeters (1988) to determine coefficients a , b and c . Following this, light curve parameters of relative maximum electron transport rate ($rETR_{max}$), coefficient of light use efficiency (α) and light saturation coefficient (E_k) were calculated from the parameters a , b and c following the equations in Eilers and Peeters (1988). The software used for curve fitting and regression analysis to determine curve parameters was Sigmaplot V11. Non-photochemical quenching (NPQ) was calculated as the change in maximum fluorescence yield ($NPQ = (F_m - F_m')/F_m'$), where F_m was taken as the initial value recorded in the rapid light curve (e.g. after 30 seconds of darkness).

Pigment analysis

Approximately 50 mg of freeze-dried sediment were extracted in 95% cold buffered methanol (2% ammonium acetate) for 15 min at -20°C , in the dark. Samples were sonicated (Bransonic, model 1210) for 30 s at the beginning of the extraction period. Extracts were filtered (Fluoropore PTFE filter membranes, 0.2 μm pore size) and immediately injected in a Shimadzu HPLC with photodiode array and fluorescence (Ex. 430 nm; Em. 670 nm) detectors (Cartaxana and Brotas, 2003). Chromatographic separation was carried out using a C18 column for reverse phase chromatography

(Supelcosil; 25 cm long; 4.6 mm in diameter; 5 μ m particles) and a 35 min elution programme. The solvent gradient followed Kraay et al. (1992) with a flow rate of 0.6 mL min⁻¹ and an injection volume of 100 μ L. Pigments were identified from absorbance spectra and retention times and concentrations calculated from the signals in the photodiode array detector or fluorescence detectors. Calibration of the HPLC peaks was performed using commercial standards from Sigma-Aldrich and DHI (Institute for Water and Environment). Samples were analysed for the xanthophyll pigments DD (the epoxidised form) and DT (the de-epoxidised form). The state of de-epoxidation (DEP in %) was calculated as $DT/(DD+DT) \times 100\%$.

Radiolabelled carbon uptake

Total primary productivity (μ g C [μ g Chl *a*]⁻¹ h⁻¹) was measured from subsamples of ¹⁴C-labelled biofilm. Minicores were incubated *in situ* with labelled ¹⁴C sodium bicarbonate. One mL (370 Bq) of label was added to each core and allowed to diffuse in the dark for 30 min. After dark diffusion (Smith and Underwood 1998) a 30 min incubation was carried out in both the ambient light and the constant light treatments, terminated by addition of 5% gluteraldehyde. The surface 2 mm depth (approximately) of each minicore was extracted and transferred to an Eppendorf. Sediment samples were later freeze-dried and had inorganic label driven off by addition of concentrated HCl for 24 h. After addition of scintillant cocktail (Optiphase Safe, Fisons, Loughborough, UK), carbon uptake rates were calculated from counts obtained from a Packard Tricarb460C scintillation counter (LKB, Cambridge, UK) with internal quench correction. Counts

were corrected for self-quenching by the sediment using radiation standard curves with and without sediment addition. Self quenching reduced counts by 2 to 5%.

Statistical analysis

Significant difference was determined using two factor ANOVA with chemical treatment (Lat A, DTT or controls) nested within light treatment (ambient or constant light) nested within time (T1, 2, and 3). This resulted in 3 replicates for each of the 3 chemical treatments nested within 2 light treatments within 3 time points. Normality and homogeneity of variance of data were tested using the Kolmogorov-Smirnov test followed by Bartlett's or Levene's test (for normal or non normal data respectively). If data did not have equal variance then a log transformation was applied (Zar, 1999). In all cases data were normal and non-parametric testing was not required. All tests were applied using Minitab V15 software.

Results

Accumulated light dose

The light dose calculated for ambient light and the constant light treatment (Table 2), showed a slightly higher accumulated dose for the constant light treatment at T1, which was reversed by T2. However it was not until T3 that the difference in light dose between the two treatments was significantly large, with a light dose under ambient light being 2.6 times that under constant light.

Migration

Visual observation of the biofilms showed clear downward migration of cells over the experimental time period except for the Lat A treatment which showed no difference in appearance (Authors pers. obs.). This was largely corroborated by the pigment data (Chl *a*) which showed clear declines in surface biomass by time T3 (**Figure 1**) for controls and DTT treatments under constant light ($F_{2,26} = 25.90$, $p < 0.01$) and under ambient light ($F_{2,26} = 14.05$, $p < 0.01$), but with no pattern of decline for the Lat A treatment. Migration monitored using the spectral reflectance NDVI index (**Figure 2**) showed a similar result, with a decrease in surface biomass under ambient light for all three chemical treatments ($F_{2,26} = 23.4$, $p < 0.01$) between T2 and T3, although the percentage decline for Lat A was only half that of the DTT treatment and the controls. Under constant light, no data were obtained for T1, however between T2 and T3 there was a significant ($F_{2,17} = 18.6$, $p < 0.05$) decline for the controls and DTT treatment, but no decline for the Lat A treatment. Overall, the Lat A clearly inhibited cell vertical migration compared to the other two treatments.

Fluorescence data

There was a significant decrease ($F_{2,26} = 8.403$, $p < 0.01$) in $rETR_{max}$ over the experimental period for all treatments, although the magnitude of the decline was lower in treatments under constant light compared to those under higher ambient light (**Figure 3**). There was no significant difference in $rETR_{max}$ between treatments at time T1 or T2, however by T3 the Lat A treatment showed a significantly lower ($F_{2,26} = 7.444$, $p < 0.05$) value than controls and the DTT treatment for both light treatments. The magnitude of this difference was clearly larger under ambient light compared to constant light. There

was no significant difference between controls and the DTT treatment under either light environment.

Under constant light, α showed no significant pattern over time (**Figure 4**), although in general slight decreases (noticeable most for the DTT treatment) were observed. However under ambient light, α significantly decreased ($F_{2,26} = 6.281$, $p < 0.05$) in all three treatments, with the decrease for the Lat A treatment being significantly greater ($F_{2,26} = 6.810$, $p < 0.05$) than either controls or DTT treatments. The value for the Lat A treatment at T3 was essentially zero (0.0005 rel. units compared to an initial value of 0.25 real. units). The light saturation coefficient (E_k) followed exactly the same patterns as described above for $rETR_{max}$, due to the magnitude of change in $rETR_{max}$ dominating the shape of the light response curves, rather than that of α (note $E_k = rETR_{max} / \alpha$).

Productivity (^{14}C uptake rate)

Due to a high level of variation in values between replicates of the same treatment, no significant differences were observed between chemical treatments in either ambient light or constant light (**Figure 5**). There was also no significant difference between light treatments, however over time, all data showed a significant decrease ($F_{2,26} = 15.08$, $p < 0.01$). Productivity did not correlate with $rETR_{max}$ uptake within chemical treatments, although the temporal decline for all data showed a significant correlation ($r = 0.63$, $n = 27$, $p < 0.05$) with $rETR_{max}$ (**Figure 6**). It should be noted that the ^{14}C has a lower resolution than the fluorescence methodology, with measurements effectively integrated over the surface 5 mm of the sediment rather than restricted to surface and near surface analysis for the latter method.

Non photochemical quenching (NPQ)

NPQ calculated from the change in maximum fluorescence yield $(F_m - F_m')/F_m'$, surprisingly showed negligible induction. In all cases the decline in quantum efficiency $(\Delta F/F_m')$ was the result of an increase in F' relative to F_m' (**Figure 7**), F_m' initially declined before showing an asymptotic increase. Such a pattern resulted in small values of NPQ (< 0.20) at low light, followed by a decrease to near zero, or often less than zero, at light levels at and above $320 \mu\text{mol m}^{-2} \text{s}^{-1}$ PAR (data not shown). DT measured by spectral analysis showed little change in the three treatments by T1 and T2 (**Figure 8**), however by T3 the DTI values were greater for the non-migratory Lat A treatment compared to the migratory biofilms in both controls and the DTT treatments. This method is under development, but clearly shows a treatment effect for the Lat A treatment regarding NPQ induction compared to the other two treatments. This overall pattern was corroborated by concomitant samples analysed by pigment analysis (**Figure 9**). Data for pigment analysis expressed as DD de-epoxidation (%), DT/Chl *a* and DT+DD/Chl *a* are shown in comparison with corresponding spectral derivative analysis. These data showed little (non-significant) change under constant low light, however under high light, both DD de-epoxidation and DT/Chl *a* showed significantly higher values by T3 ($F_{2,26} = 157.67$ $p < 0.001$) for the Lat A treatments compared to controls and the DTT treatment.

Discussion

These data clearly indicate that, for these biofilms at least, benthic diatoms principally employ vertical migration as their first main mechanism in response to increasing light dose exposure. This is concluded from the significant photoinhibition of the Lat A treated biofilms, with probable enhanced level of physiological down regulation through NPQ, when compared to the two migratory treatments, DTT treated biofilms and controls. In simple terms, cells migrated vertically in response to increasing light dose over time, but when vertical movement was inhibited by Lat A, NPQ induction increased, but not sufficiently to prevent photoinhibition. This is in agreement with the light induced vertical movement (microcycling) proposed by Kromkamp et al. (1998), Serôdio and Catarino (1999) and Perkins et al. (2002), and also further emphasises the role of vertical movement demonstrated in other experiments using the same chemical inhibitors (Cartaxana and Serôdio 2008; Cartaxana et al. 2008).

Migration was significantly inhibited by the addition of Lat A (Figures 1 and 2), in agreement with work by Cartaxana et al. (2008) and Cartaxana and Serôdio (2008). This was apparent through analysis of Chl *a* pigment in the surface 2 mm (a comparatively low resolution method) and the surface chlorophyll proxy, NDVI. Both methods showed no major change over the experimental period, whereas for controls and the DTT treated biofilms, significant decreases in biomass were observed. It should be noted that there was no significant difference in biomass between DTT treatment and controls, indicating that DTT did not induce an increase or decrease in cell movement relative to controls. It should also be noted that patterns were largely the same between ambient light and constant light, thus the magnitude of the photodose did not enhance

417 migration. This latter point could have two explanations. Firstly the magnitude of the
418 vertical migration may have been predominantly determined by an endogenous tidal
419 rhythm (e.g. Serôdio et al. 1997) rather than the light dose. Secondly micro-cycling of
420 cells (Kromkamp et al. 1998; Perkins et al. 2002) may have resulted in similar light dose
421 exposure, irrespective of the two light treatments. Thus the integrated light dose of cells
422 cycling through the surface of the sediment was not significantly greater in the ambient
423 light treatment (this being the product of light intensity and length of exposure) compared
424 to cells at lower light level in the constant light treatment. It is likely that both processes
425 played a role in the migratory pattern of the controls and DTT treated cells, however
426 differentiation between these two driving functions was not an explicit aim of this study.
427 Also it should be noted that comparison of ambient light data at T2 and constant light
428 data at T3, which related to biofilms that had been exposed to similar overall light dose,
429 showed subtle differences in fluorescence values ($rETR_{max}$ and α), demonstrating that
430 light dose was not the sole driving function of the differences observed. Furthermore
431 NPQ induction were investigated over the 6 h emersion period and hence the resolution
432 of the measurements did not analyse short term patterns in NPQ induction. It is well
433 known that diatoms may rapidly induce NPQ in response to short term (10s of seconds)
434 changes in light environment (e.g. Perkins et al. 2006). The role of the comparatively
435 long term light dose effect can be noted by the fact that it was not until T3, when the
436 difference in light dose between the two treatments was greatest (Table 2), that
437 differences between the chemical treatments were of highest magnitude.

438 Over the exposure period, relative maximum electron transport rate ($rETR_{max}$)
439 decreased in all treatments (Figure 3). This may have been the result of an endogenous

diel rhythm (Underwood et al. 2005) and / or the effect of the increasing photodose. As the magnitude of the decrease was greatest under ambient light, compared to the lower photodose experienced under constant light, both an endogenous decrease and a photodose effect seem likely. The magnitude of this decrease in $rETR_{max}$ was greatest for Lat A treated biofilms, but only significantly so under ambient light, indicating the inhibition of cell vertical movement resulted in photoinhibition. This pattern was also indicated by the decline to effectively zero by the light use efficiency coefficient (α) for the Lat A treated biofilms under ambient light (Figure 4). Clearly this higher photodose induced photoinhibition (possibly photodamage) when cells were unable to migrate away from the sediment surface. It should be noted that no difference was observed between the DTT treated biofilms and the controls. Therefore it can be concluded that inhibition of NPQ (DTT treatment) had no significant impact whereas inhibition of migration (Lat A treatment) resulted in a reduction in both $rETR_{max}$ and α , but only when the light dose was sufficiently high compared to the constant light treatment.

It is unlikely that the decrease in photosynthetic activity over the experimental period was the result of increasing environmental stress in response to experimental conditions. In fact the use of the water bath may have reduced temperature stress relative to in situ temperature increases, and the biofilms showed no obvious drying out for any of the treatments. In situ warming and desiccation are likely to be equal to or greater than those experienced during this study, thus any temporal pattern is likely to occur under in situ conditions as well. In addition, as all chemical treatments were exposed to the same stress, albeit a lower warming under constant light, experimental induced stresses cannot explain the differences between the Lat A treatment and the controls and DTT treatment.

Productivity, when measured by ^{14}C uptake rate, showed no chemical or light treatment effects, indeed the only significant pattern observed was an overall temporal decline over the experimental period for the whole dataset. This decline correlated with that of rETR_{max} (Figure 6) supporting the statement above that a combination of diel rhythm and light dose exposure resulted in a decrease in photosynthetic activity. The lack of any chemical treatment effect could be due to two reasons. Firstly the method effectively integrates the productivity measurement over the surface 5 mm depth of sediment, hence resulting in a weighted average value dependent upon the biomass distribution over this depth. Secondly the chemical treatments may not have been fully active at depth despite the pre-measurement 30 minute incubation period, hence resulting in cell migration towards the surface of cells able to replenish the surface biofilm with photosynthetically active cells. The former seems more probable as an explanation as the latter would have resulted in a surface biomass enrichment in the Lat A treatment (i.e. cells would have migrated to the surface and then been unable to migrate back down due to the chemical treatment), which was not observed.

Analysis of the data indicating induction of non-photochemical quenching (NPQ) is not so clear cut. In all biofilms, the quenching of the photochemical efficiency ($\Delta F/F_m'$) was the result of an increase in F' and not a quenching of the F_m' yield. This indicates a low level or even lack of induction of NPQ as indicated by the calculated values ($\text{NPQ} = (F_m - F_m')/F_m'$). For the migratory biofilms the data must be interpreted with care as downward migration between measurements of F_m and F_m' results in an increase in the calculated value of NPQ solely due to the increased distance between the cells and the fluorimeter probe (e.g. Consalvey et al. 2005; Perkins et al. in press).

However this would have increased the magnitude in difference between the non-migratory (Lat A) and migratory (controls and DTT) treatments. In comparison, both the spectral derivative (Figure 8) and the pigment analysis (Figure 9) for biofilms under ambient light indicated a greater level of NPQ induction in the Lat A treated biofilms. Under constant light there was no difference between controls and DTT treated biofilms and no difference between chemical treatments. Thus a photodose effect was observed whereby the higher ambient light photodose induced a greater level of NPQ when cell vertical movement was inhibited. Diadinoxanthin de-epoxidation as well as the relative Diatoxanthin (DT) concentration (DT/Chl *a*) both showed the same patterns. Interestingly there was no increase in (DD+DT) concentration, indicating no de novo synthesis but a conversion of DD to DT as the primary NPQ mechanism. This is an expected result in response to high light exposure (Lavaud et al., 2004; Schumann et al. 2007). The lack of any significant effect of DTT treatment compared to controls may imply that the DTT dose was insufficient to inhibit NPQ induction. Certainly under ambient light, pigment data show an induction of NPQ in both these treatments relative to the constant light treatment. However the spectral derivate did not show this pattern, nor did fluorescence data indicate NPQ induction for any treatment. In addition the magnitude of NPQ induction in controls and DTT treatments was significantly less than in the Lat A treatment. Therefore the overall pattern in the combined datasets indicate that cell vertical movement was more important in optimizing photosynthetic activity, rather than NPQ induction.

In conclusion, this study has two main findings. Firstly optimization of photosynthetic activity in response to an increasing exposure to light (i.e. an accumulated

light dose response) is largely due to vertical cell migration. Cells position themselves in the sediment surface layer such that the attenuation of light provides an optimal light environment for their photochemistry. This is in agreement of the microcycling and light induced vertical migration responses reported by Kromkamp et al. (1998), Serodio and Catarino (2000) and Perkins et al. (2002). In addition, it goes towards explaining the fact that integrated biofilm light response curves examined in literature seem to saturate at 400 – 800 $\mu\text{mol m}^{-2} \text{s}^{-1}$ PAR (see Perkins et al., 2002, 2006; Serôdio et al., 2003; Consalvey et al., 2005; Jesus et al., 2005, 2006 and others), significantly lower than ambient light levels at the sediment surface on a sunny day. It seems logical then that cells would position themselves in a light environment nearer to 800 $\mu\text{mol m}^{-2} \text{s}^{-1}$ PAR or lower, rather than expose themselves to the potentially photodamaging light intensities at the sediment surface. This cell migration may well be more energetically favorable than physiological down regulation processes such as NPQ induction. It is hypothesized from this data that NPQ is a secondary response to light dose and / or a response to more rapid changes in light environment rather than a longer term increase in light dose. Secondly these data suggest that a probable combination of vertical migration and physiological mechanisms result in a diel and/or tidal pattern of down regulation. Underwood et al. (2005) reported diel down regulation at the single cell level, and other studies suggest probable tidal patterns for integrated biofilm measurements (Perkins et al., 2001; Jesus et al., 2005, 2006). Again it is logical that after adequate light exposure for photosynthate production, cells would down regulate their photosynthetic activity. Hence this diel pattern may be a response to integration of the light dose over time, rather than an endogenous rhythm. Hence this study has shown overall, the importance of cell vertical

532 movement as a driving function optimizing photosynthetic activity in response to light
533 dose for benthic biofilms dominated by diatoms.

534

535 **References**

- 536 Brotas V, Cabrita T, Portugal A, Serôdio J, Catarino F (1995) Spatio-temporal distribution
537 of the microphytobenthic biomass in intertidal flats of Tagus Estuary (Portugal).
538 Hydrobiologia 300/301:93-104.
- 539 Cartaxana P, Brotas V (2003) Effects of extraction on HPLC quantification of major
540 pigments from benthic microalgae. Archiv Hydrobiol 157: 339-349.
- 541 Cartaxana P, Serôdio J (2008) Inhibiting diatom motility: a new tool for the study of the
542 photophysiology of intertidal microphytobenthic biofilms. Limnol Oceanogr Meth 6:466-
543 476.
- 544 Cartaxana P, Brotas V, Serôdio J (2008) Effects of two motility inhibitors on the
545 photosynthetic activity of the diatoms *Cylindrotheca closterium* and *Pleurosigma*
546 *angulatum*. Diatom Res 23: 65-74.
- 547 Consalvey M, Paterson DM, Underwood GJC (2004) The ups and downs of life in a
548 benthic biofilm: Migration of benthic diatoms. Diatom Res 19:181-202
- 549 Consalvey M, Perkins RG, Underwood GJC, Paterson DM (2005) PAM Fluorescence: A
550 beginners guide for benthic diatomists. Diatom Res 20:1-22.
- 551 Cruz S, Serodio J (2008) Relationship of rapid light curves of variable fluorescence to
552 photoacclimation and non-photochemical quenching in a benthic diatom. Aquat Bot 88:
553 256-264
- 554 Eilers PCH, Peeters JCH (1988) A model for the relationship between light intensity and
555 the rate of photosynthesis in phytoplankton. Ecol Model 42:199-215.

556 Forster RM, Jesus B (2006) Field spectroscopy of estuarine intertidal sediments. *Int J*
 557 *Remote Sens* 27:3657-3669.

558 Goss R, Ann Pinto E, Wilhelm C, Richter M (2006) The importance of a highly active
 559 and ΔpH -regulated diatoxanthin epoxidase for the regulation of the PS II antenna
 560 function in diadinoxanthin cycle containing algae. *J Plant Physiol* 163:1008-1021.

561 Jesus B, Brotas V, Marani M, Paterson DM (2005) Spatial dynamics of
 562 microphytobenthos determined by PAM fluorescence. *Estuar Coast Shelf Sci* 65: 30-42.

563 Jesus B, Perkins RG, Consalvey M, Brotas V, Paterson DM, (2006a) Effects of vertical
 564 migrations by benthic microalgae on fluorescence measurements of photophysiology.
 565 *Mar Ecol Prog Ser* 315:55-66.

566 Jesus B, Perkins RG, Mendes CR, Brotas V, Paterson DM (2006b) Chlorophyll
 567 fluorescence as a proxy for microphytobenthic biomass: alternatives to the current
 568 methodology. *Mar Biol* 150:17-28.

569 Jesus B, Mendes CR, Brotas V, Paterson DM (2006c) Effect of sediment type on
 570 microphytobenthos vertical distribution: Modelling the productive biomass and
 571 improving ground truth measurements. *J Exp Mar Biol Ecol* 332:60-74.

572 Jesus B, Mouget JL, Perkins RG (2008) Detection of diatom xanthophyll cycle using
 573 spectral reflectance *J Phycol* 44:1349-1359.

574 Kraay GW, Zapata M, Veldhuis M (1992) Separation of chlorophylls c_1 , c_2 , and c_3 of
 575 marine phytoplankton by reversed-phase C18 high-performance liquid chromatography.
 576 *J. Phycol.* 28:708-12.

577 Kromkamp J, Barranguet C, Peene J (1998) Determination of microphytobenthos PSII
 578 quantum efficiency and photosynthetic activity by means of variable chlorophyll
 579 fluorescence. *Mar Ecol Prog Ser* 162:45-55.

580 Lavaud J (2007) Fast regulation of photosynthesis in diatoms: Mechanisms, evolution
 581 and ecophysiology. *Funct Plant Sci Biotech* 1:267-287.

582 Lavaud J, van Gorkom H, Etienne A (2002a) Photosystem II electron transfer cycle and
 583 chlorespiration in planktonic diatoms. *Photosynth Res* 74: 51-59.

584 Lavaud J, Rousseau B, van Gorkom H, Etienne A-L (2002b) Influence of the
 585 diadinoxanthin pool size on photoprotection in the marine planktonic diatom
 586 *Phaeodactylum tricornutum*. *Plant Physiol* 129:1398-1406.

587 Lavaud J, Rousseau B, Etienne A-L (2004) General features of photoprotection by energy
 588 dissipation in planktonic diatoms (Bacillariophyceae). *J Phycol* 40:130-137.

589 Louchard EM, Reid P, Stephens CF, Davis CO, Leathers RA, Downs TV, Maffione R
 590 (2002) Derivative analysis of absorption features in hyperspectral remote sensing data of
 591 carbonate sediments. *Opt Express* 10:1573-1802.

592 MacIntyre HL, Geider RJ, Miller DC (1996) Microphytobenthos: the ecological role of
 593 the “Secret Garden” of unvegetated, shallow-water marine habitats. I. Distribution,
 594 abundance and primary production. *Estuaries* 19:186-201.

595 Materna AC, Sturm S, Kroth PG, Lavaud J (2009) First induced plastid genome
 596 mutations in an alga with secondary plastids: *psbA* mutations in the diatom
 597 *Phaeodactylum tricornutum* (Bacillariohyceae) reveal consequences on the regulation of
 598 photosynthesis. *J Phycol* 45:838-846.

599 Mouget J-L, Perkins RG, Consalvey, M, Lefebvre S (2008) Migration or
600 photoacclimation to prevent photoinhibition and UV-B damage in marine
601 microphytobenthic communities. *Aquatic Microbial Ecology*, 52 : 223-232.

602 Olaizola M, Laroche J, Kolber Z, Falkowski PG (1994) Non-photochemical fluorescence
603 quenching and the diadinoxanthin cycle in a marine diatom. *Photosynth Res* 41:357-370.

604 Perkins RG, Kromkamp JC, Serôdio J, Lavaud J, Jesus BM, Mouget J-L, Lefebvre S,
605 Forster RM. In Press. The application of variable chlorophyll fluorescence to
606 microphytobenthic biofilms.

607 Perkins RG, Underwood GJC, Brotas V, Snow GC, Jesus B, Ribeiro L (2001) Responses
608 of microphytobenthos to light: primary production and carbohydrate allocation over an
609 emersion period. *Mar Ecol Prog Ser* 223:101-112.

610 Perkins RG, Oxborough K, Hanlon ARM, Underwood GJC, Baker NR (2002) Can
611 chlorophyll fluorescence be used to estimate the rate of photosynthetic electron transport
612 within microphytobenthic biofilms? *Mar Ecol Prog Ser* 228:47-56.

613 Perkins R, Mouget J-L, Lefebvre S, Lavaud J (2006) Light response curve methodology
614 and possible implications in the application of chlorophyll fluorescence to benthic
615 diatoms. *Mar Biol* 149:703-712.

616 Pinckney J, Zingmark R (1991) Effects of tidal stage and sun angles on intertidal benthic
617 microalgal productivity. *Mar Ecol Prog Ser* 76:81-89.

618 Ruban A, Lavaud J, Rosseau B, Guglielmi G, Etienne A (2004) The super-excess energy
619 dissipation in diatom algae: comparative analysis with higher plants. *Photosynth Res*
620 82:65-175.

621 Schumann A, Goss R, Jakob T, Wilhelm C (2007) Investigation of the quenching
 622 efficiency of diadinoxanthin in cells of *Phaeodactylum tricornutum* (Bacillariophyceae)
 623 with different pool sizes of xanthophyll cycle pigments. *Phycologia* 46:113-117.

624 Serôdio J, da Silva JM, Catarino F (1997) Non destructive tracing of migratory rhythms
 625 of intertidal benthic microalgae using *in vivo* chlorophyll *a* fluorescence. *J Phycol*
 626 33:542-553.

627 Serôdio J, Catarino F (1999) Fortnightly light and temperature variability in estuarine
 628 intertidal sediments and implications for microphytobenthos primary productivity. *Aquat*
 629 *Ecol* 33:235-241

630 Serôdio J, Cruz S, Vieira S, Brotas V (2005) Non-photochemical quenching of
 631 chlorophyll fluorescence and operation of the xanthophyll cycle in estuarine
 632 microphytobenthos. *J Exp Mar Biol Ecol* 326: 157-169

633 Serôdio J, Vieira S, Cruz S (2008) Photosynthetic activity, photoprotection and
 634 photoinhibition in intertidal microphytobenthos as studied in situ using variable
 635 chlorophyll fluorescence. *Cont Shelf Res* 28: 1363-1375

636 Spilmont N, Migne A, Seuront L, Davoult D (2007) Short-term variability of intertidal
 637 benthic community production during emersion and the implication in annual budget
 638 calculation. *Mar Ecol Prog Ser* 333:95 – 101

639 Ting CS, Owens TG (1993) Photochemical and non-photochemical fluorescence
 640 quenching processes in the diatom *Phaeodactylum tricornutum*. *Plant Physiol* 101:1323-
 641 1330.

642 Underwood GJC, Kromkamp J (1999) Primary production by phytoplankton and

643 microphytobenthos in estuaries. *Adv Ecol Res* 29: 93-153.

644 Underwood GJC, Perkins RG, Consalvey M, Hanlon ARM, Oxborough K, Baker NR,
645 Paterson DM (2005) Patterns in microphytobenthic primary productivity: Species-
646 specific variation in migratory rhythms and photosynthetic efficiency in mixed-species
647 biofilms. *Limnol Oceanogr* 50:755-767.

648 Zar JH (1999) *Biostatistical Analysis*, 4th edn. Prentice Hall, Upper Saddle River, NJ.

Table 1. Overview of the experimental design showing the nesting of chemical treatments (Lat A = Latrunculin A to inhibit cell motility; DTT = DL-dithiothreitol to inhibit NPQ and controls) within light treatment (Amb = ambient, Con = constant) within time period (T1, 2, and 3) and the measurements made (Spec = spectroradiometry to measure NPQ induction and surface biomass as NDVI, RLC = rapid light curve by fluorescence, Pig = pigments including Chl a, DD and DT, ^{14}C = productivity measured as labelled carbon uptake rate). All measurements were made as triple replicates, i.e. 3 separate minicores.

Time period	Light Treatment	Chemical treatment	Measurement, minicore set 1	Measurement, minicore set 2
T1	Amb	Lat A	Spec, RLC, Pig	^{14}C
		DTT	Spec, RLC, Pig	^{14}C
		Controls	Spec, RLC, Pig	^{14}C
	Con	Lat A	Spec, RLC, Pig	^{14}C
		DTT	Spec, RLC, Pig	^{14}C
		Controls	Spec, RLC, Pig	^{14}C
T2	Amb	Lat A	Spec, RLC, Pig	^{14}C
		DTT	Spec, RLC, Pig	^{14}C
		Controls	Spec, RLC, Pig	^{14}C
	Con	Lat A	Spec, RLC, Pig	^{14}C
		DTT	Spec, RLC, Pig	^{14}C
		Controls	Spec, RLC, Pig	^{14}C
T3	Amb	Lat A	Spec, RLC, Pig	^{14}C
		DTT	Spec, RLC, Pig	^{14}C
		Controls	Spec, RLC, Pig	^{14}C
	Con	Lat A	Spec, RLC, Pig	^{14}C
		DTT	Spec, RLC, Pig	^{14}C
		Controls	Spec, RLC, Pig	^{14}C

662

663

664 Table 2. Accumulated light dose calculated from the product of light measurement and
665 length of exposure at each sampling time (T1, T2 and T3) for the ambient and constant
666 light treatments. Units of light dose are mole of photons m⁻².

667

Sampling Time	Ambient treatment light dose	Constant treatment light dose
T1	1.82	2.16
T2	7.83	5.40
T3	20.00	7.56

668

669

670

Figure legends

Figure 1. Biomass represented as the proxy of chlorophyll a (Chl a) for each chemical (D = DTT, L = Lat A, C = control) and light treatment (Amb = ambient, Con = constant) over the three sampling points (T1, T2 and T3). Values are mean \pm s.e. (n = 3).

Figure 2. Surface biomass represented as the proxy of Normalised Difference Vegetation Index (NDVI) measured using the spectroradiometer. Values are represented as percentage change compared to the initial value at T1 for each chemical (D = DTT, L = Lat A, C = control) and light treatment (Amb = ambient, Con = constant) over the three sampling points (T1, T2 and T3). Values are mean \pm s.e (n = 3).

Figure 3. Maximum relative electron transport ($rETR_{max}$) rate as a proxy for productivity measured using variable chlorophyll fluorescence. Values are represented as percentage change compared to the initial value at T1 for each chemical (D = DTT, L = Lat A, C = control) and light treatment (Amb = ambient, Con = constant) over the three sampling points (T1, T2 and T3). Values are mean \pm s.e (n = 3).

Figure 4. Light utilisation coefficient (α) measured using variable chlorophyll fluorescence. Values are represented as percentage change compared to the initial value at T1 for each chemical (D = DTT, L = Lat A, C = control) and light treatment (Amb = ambient, Con = constant) over the three sampling points (T1, T2 and T3). Values are mean \pm s.e (n = 3).

Figure 5. Productivity measured as the uptake rate of labelled carbon (^{14}C - NaHCO_3) for each chemical (D = DTT, L = Lat A, C = control) and light treatment (Amb = ambient, Con = constant) over the three sampling points (T1, T2 and T3). Values are mean \pm s.e (n = 3).

Figure 6. Maximum relative electron transport rate (rETR_{max}) presented as a function of productivity (^{14}C uptake rate) for the whole data set.

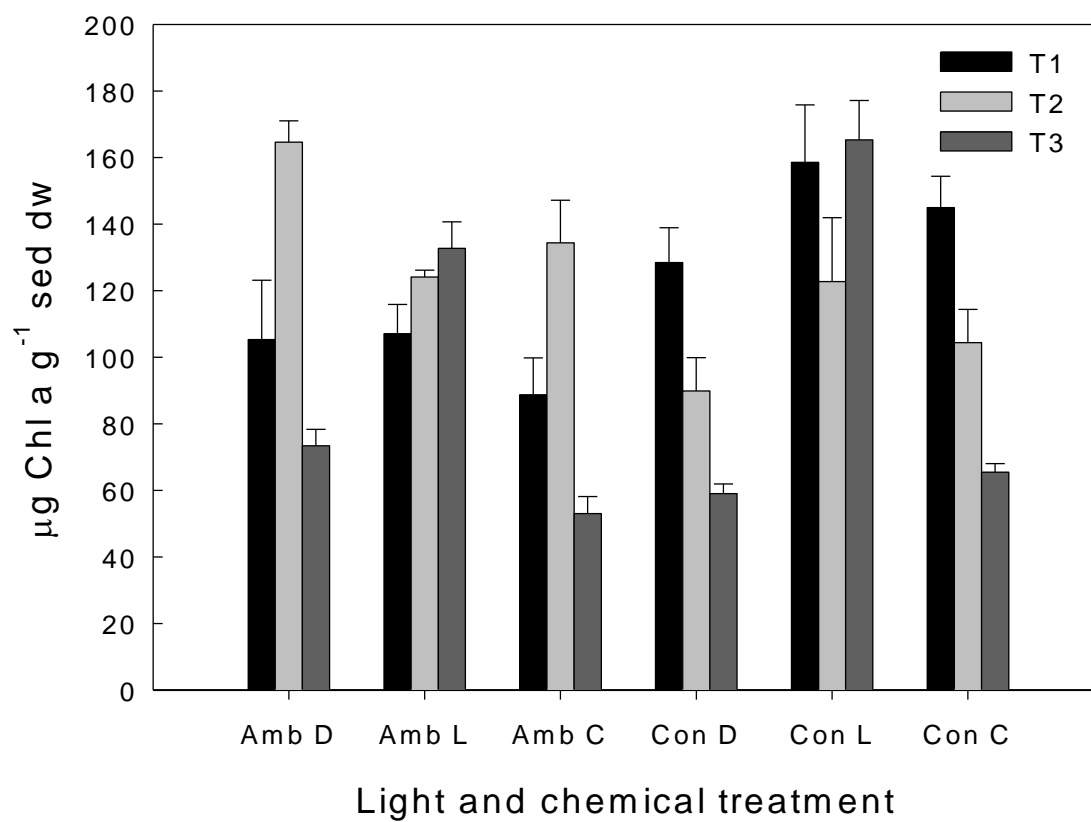
Figure 7. Operational fluorescence yield (F) and maximum fluorescence yield (F_m') during a 20 second rapid light response curve. Data shown are for a control sample, however the pattern was identical (increase in F and slight decline in F_m' followed by a curvilinear increase) for all light curves measured (all three light treatments and at all three sampling points).

Figure 8. Diatoxanthin Index measured from the spectral second derivatives (508/630 nm) for each chemical (D = DTT, L = Lat A, C = control) under the ambient light treatment (Amb = ambient) over the three sampling points (T1, T2 and T3). Values are mean \pm s.e (n = 3).

Figure 9. Pigment data of A: Diatoxanthin (DT) and the B: Percentage de-epoxidation (%) of Diadinoxanthin for each chemical (D = DTT, L = Lat A, C = control) and light treatment (Amb = ambient, Con = constant) over the three sampling points (T1, T2 and T3). Values are mean \pm s.e (n = 3).

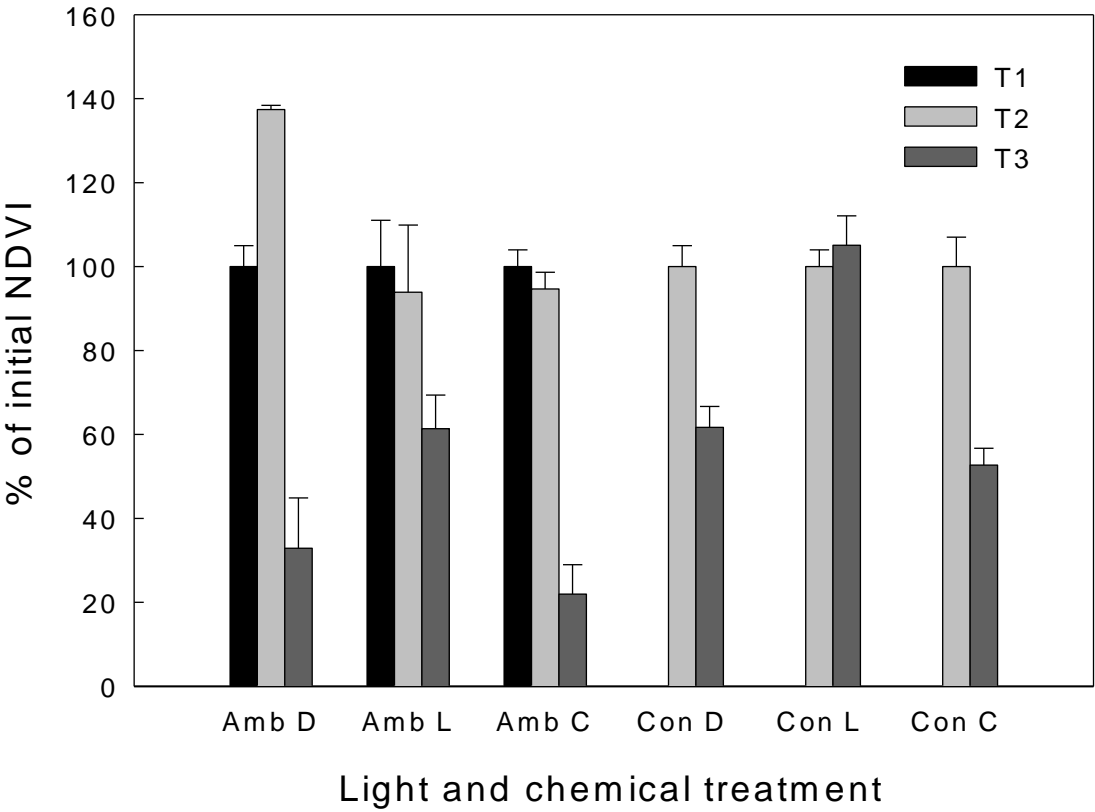
717
718

Perkins et al. Figure 1



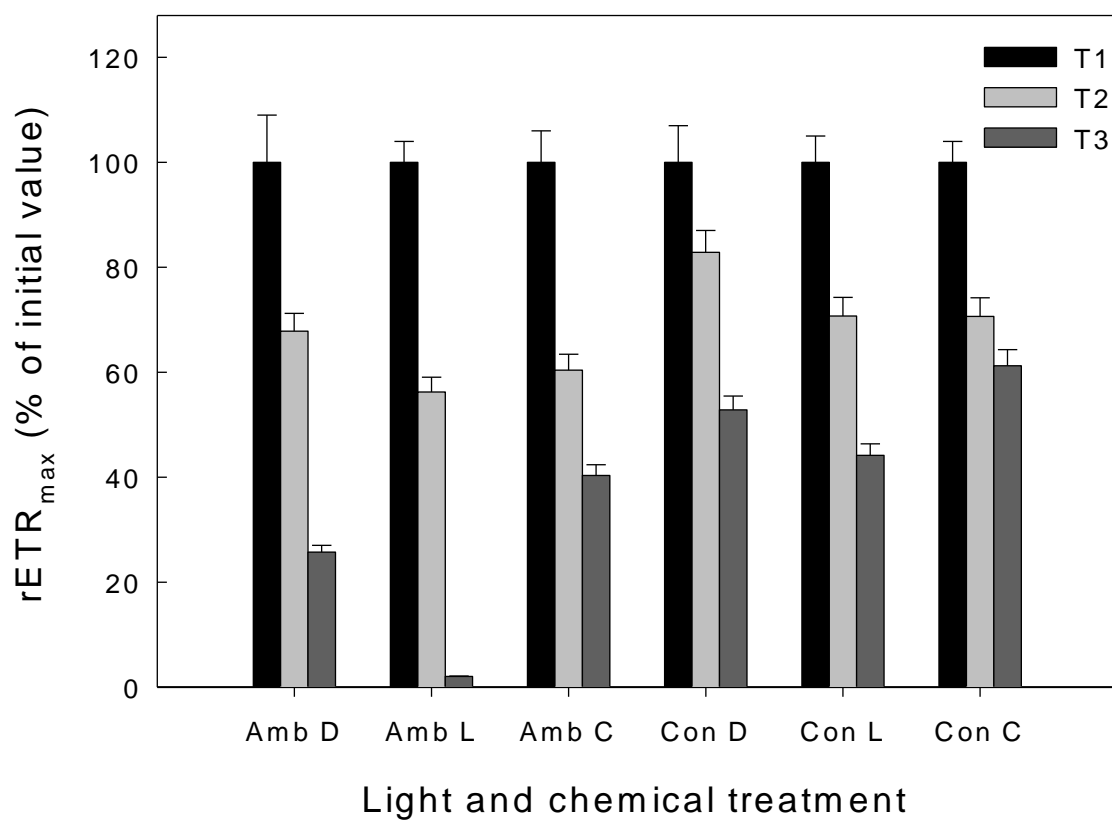
719
720
721
722
723

Perkins et al. Figure 2



724
725
726
727

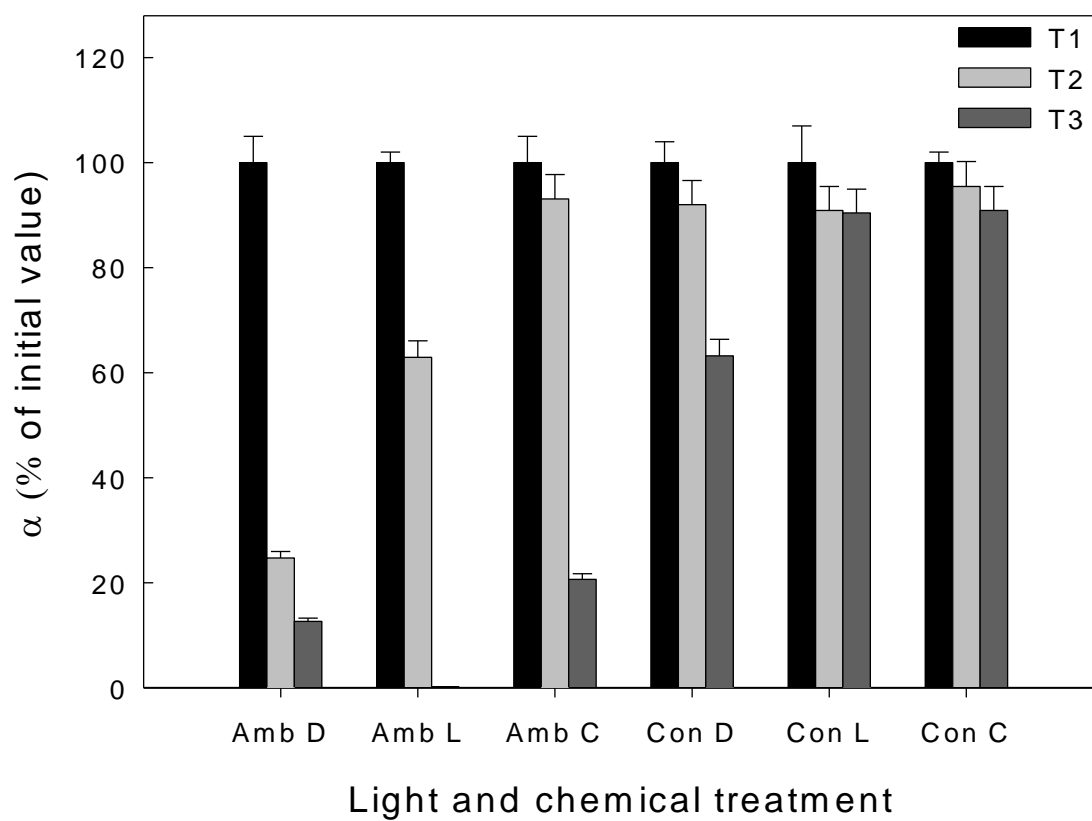
Perkins et al Figure 3



729
730
731
732
733
734

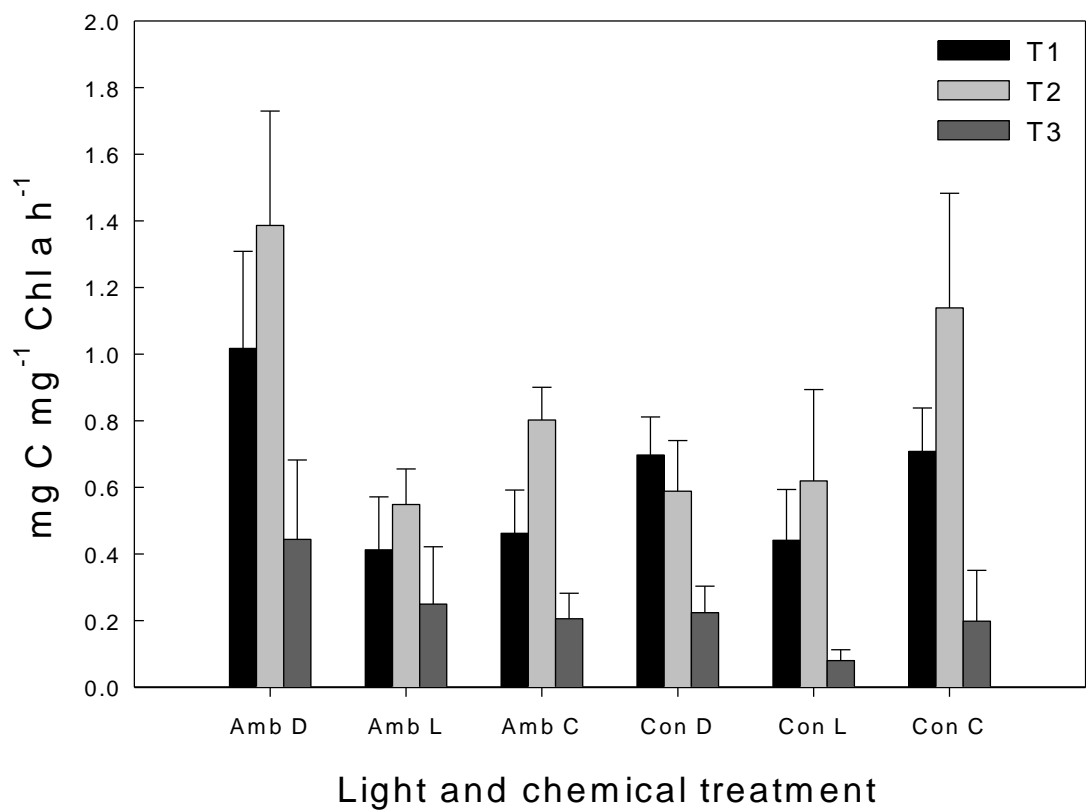
735

Perkins et al. Figure 4



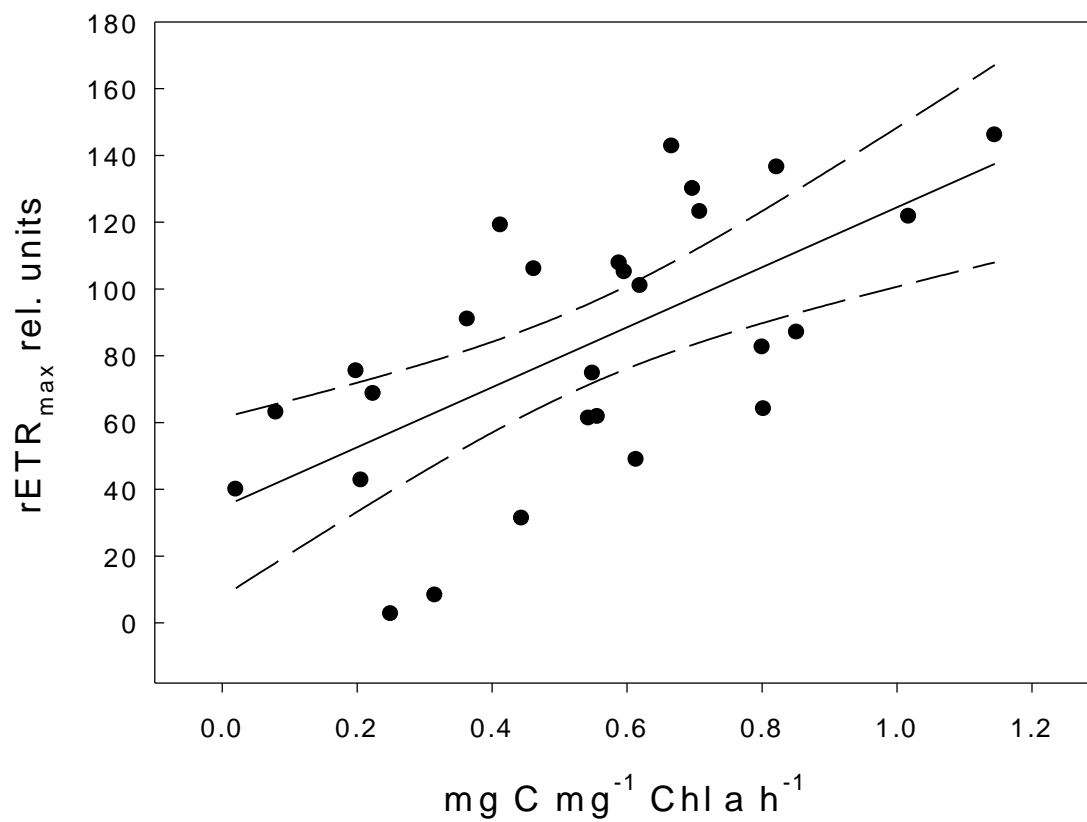
736
737
738
739
740
741
742
743

Perkins et al. Figure 5



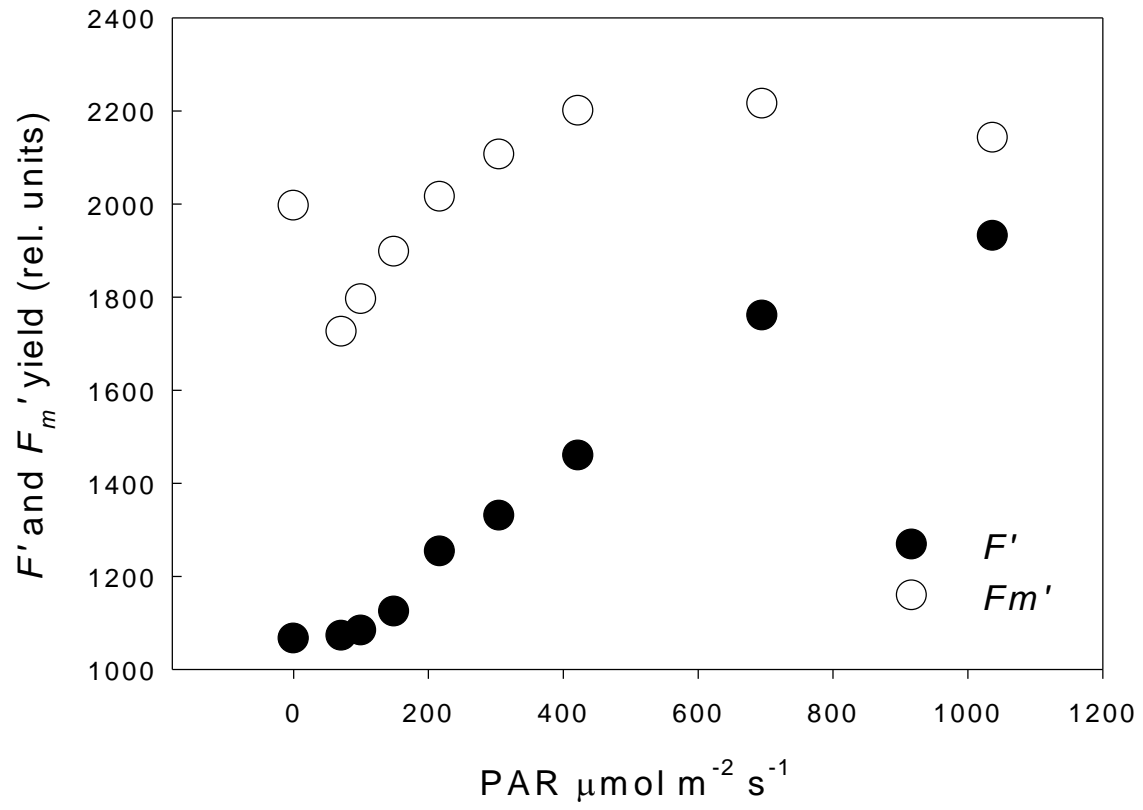
744
745
746
747
748
749

Perkins et al. Figure 6

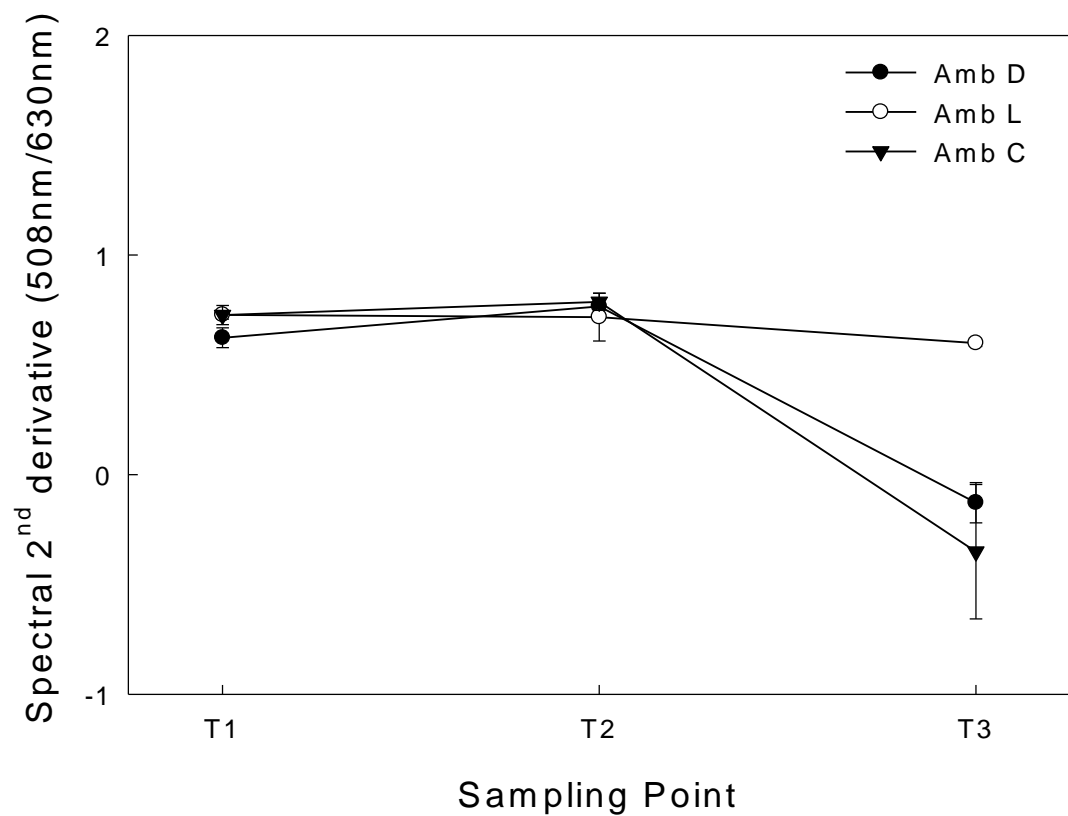


750
751
752
753
754
755

Perkins et al. Figure 7



756
757
758
759
760
761
762
763



Perkins et al. Figure 9

